International Journal of Fatigue 139 (2020) 105736

Contents lists available at ScienceDirect

International Journal of Fatigue

journal homepage: www.elsevier.com/locate/ijfatigue

Fatigue properties of steel to aluminum transition joints produced by explosion welding

Nicolas Becker[a], David Gauthier[b], Edgar E. Vidal[c,*]

[a] Institut de Soudure, 4 Boulevard Henri Becquerel, Yutz, 57970, France
[b] NobelClad, 105 rue des Frères Voisin, 66000 Perpignan, France
[c] NobelClad, 11800 Ridge Pkwy, Ste 300, Broomfield, CO 80021, USA

ARTICLE INFO

Keywords:
Explosion welding
EXW
Transition joints
Fatigue
Steel to aluminum

ABSTRACT

This manuscript presents the results of designing and testing a novel fixturing device for determining the fatigue properties of explosive bonded metals. The fatigue strength of steel to aluminum transition joints in tensile and compression stresses are presented. Additionally, shear stress for different load ratios was also studied. The stress distribution in the specimens was verified by finite element analysis. The experimental tensile/compressive fatigue results show a comparable fatigue lifetime to the recommended IIW values. The shear fatigue strength of the explosion-welded junction tested in this study is equivalent to a traditional butt welded joint.

1. Introduction

Many applications require an assembly between heterogeneous metal materials that cannot be assembled by thermal processes, due to a difference in melting temperature or due to chemical incompatibility. Explosion welding (EXW), developed in the 20th century, is a method of assembling these heterogeneous metallic materials [1–3]. Typical metal alloys that can be bonded via EXW include, titanium with steel, copper with aluminum or steel with aluminum. This type of assembly is an interesting technique for the lightening of structures. But the more the structures are lightened, the more the consideration of the fatigue strength of the welded junction is important. Little data exist on the fatigue behavior of explosion welded joints [4]. Karolczuk et al. [5] performed fatigue tests on steel-titanium assemblies with a parallel load on the interface. Other authors have also performed bending tests [6–7]. But no data is available for fatigue resistance when there is stress perpendicular to the interface. In some cases, the welded joint is also required to work under cyclic shear stress, which raises the question of the fatigue strength of the interface. The purpose of our study was to evaluate the fatigue strength of an explosion-welded steel to aluminum joint in both tensile and compression stresses perpendicular to the interface, and in shear stress for different load ratios to obtain the Goodman-Smith diagrams. For these objectives, we proposed and built a specimen design to be a representative section of the interface while remaining simple. The stress distribution in the specimens was verified by finite element analysis. The results were then compared to IIW [8] recommendations for aluminum welding.

1.1. Fabrication of transition joints by explosion welding

Explosion welding developed in the 1960 s by DuPont, is defined by European standard EN ISO 4063, and American standards AWS-EXW as a solid-state welding process. The detonation of an explosive is used to project one of the sheets called “cladder”, on the other sheet called “base metal” or “backer”. Generally speaking, the cladder is the thinnest or lightest of the two metals. The collision of both surfaces at high speed and angle creates a local plasticization of the interface, a hydrodynamic flow of gases in-between the cladder and backer referred to as “jet”, which expels the oxides and impurities. The resulting bond between the metals presents the very characteristic wavy aspect of the interface which is evidence of severe plastic deformation. [9–11]

From an industrial point of view, manufacturing begins with surface preparation by grinding or chemical etching. The prepared surfaces are then assembled face to face and held at a short distance from each other, during the so-called “pre-bonding” operation. At the shooting site, the explosive is distributed over the cladder and is armed with a priming system at the location defined as the start of the explosion (initiation point). The conditions for the explosive welding process are now set: defined by the characteristics of the explosive, the surface load used, and the gap between the sheets. These will make it possible to control the impact parameters such as speed, collision angle and pressure to obtain a quality welding. After the explosion welding process,

* Corresponding author.
E-mail addresses: n.becker@isgroupe.com (N. Becker), dgauthier@nobelclad.com (D. Gauthier), evidal@nobelclad.com (E.E. Vidal).

https://doi.org/10.1016/j.ijfatigue.2020.105736
Received 14 January 2020; Received in revised form 4 May 2020; Accepted 25 May 2020
Available online 26 May 2020
0142-1123/ © 2020 DMC Global, Inc. dba Nobelclad. Published by Elsevier Ltd. This is an open access article under the CC BY license (http://creativecommons.org/licenses/BY/4.0/).

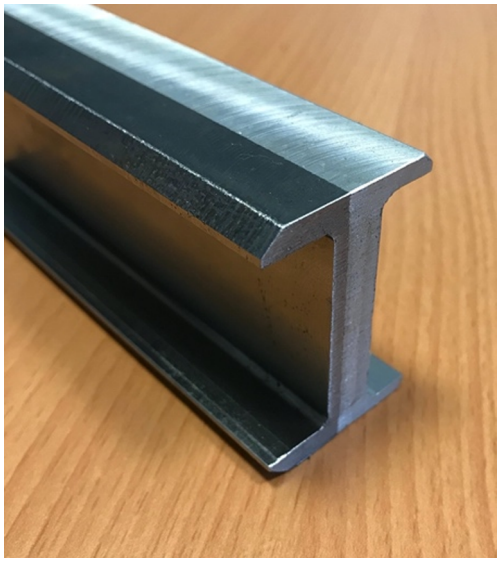

Fig. 1. Transition Joint (TJ) of aluminum (lighter) and steel (darker) machined into an "H" channel from strips cut from larger explosion welded clad plates.

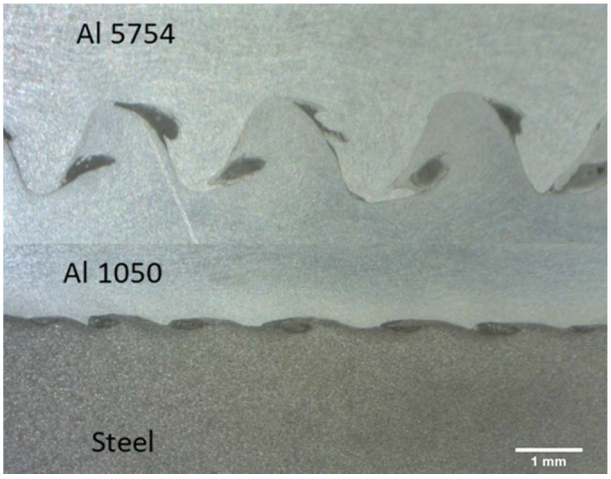

Fig. 2. Typical bond interface of a RailClad transition joint where the S355 steel backer has an interlayer of 1050-aluminum, and the 5754-aluminum cladder.

the "post-bond" operation commences. The clad plate is straightened, inspected using ultrasonic testing, cut to dimensions, marked and delivered to the customer.

1.2. Fabrication of transition joints for use in the railway industry

The plates tested in this article were developed and produced by NobelClad®. They are used in railway construction, for welding aluminum alloy decking to steel crates. As mentioned before, after the explosive welding and straightening, a 100% ultrasonic test is performed. The sheets are cut by sawing and then machined to form an "H" profile, which can be welded on both sides in a conventional manner. The result is a hybrid welded junction, permanent, lightweight, and easy to use and install. Fig. 1 shows the "H" profile which allows for welding steel plates to the steel side of the Transition Joint (TJ), and aluminum plates to the aluminum side of the TJ.

The use of steel-aluminum clad in TJs dates back to the 1960's with some fatigue studies presented by McKenney and Banker [12]. Studies like these led to the development of Military Specifications, in particular MIL-J-24459A, for use in marine shipbuilding [13] which is still relevant today. Examples of references made to the use of the "Mil Spec" making reference to the implementation of fatigue as a pass-fail criterion was presented by Moore and Banker [14] as well as Ranker and Gaines [15,16]

1.3. Characterization of the welded transition joint

The RailClad Junction is a combination of S355 steel + Al 1050 + Al 5754 (18 + 3 + 18 mm). Metallographic examination reveals a wavy-shaped interface typical of the explosive welding process. Fig. 2 shows a typical bond interface of a RailClad transition joint, where the waves between the soft 1050 aluminum interlayer and harder 5754 aluminum are significantly taller (roughly 2 mm) compared to those with the S355 steel. Swirls can be observed in both interfaces which are nothing more than re-solidified metal regions where slight variations of elemental composition exist, and likely the presence of some oxides. These regions also have solidification shrinkage which manifest in the form of pores. Fig. 3 shows the common elemental profile seen at the steel to aluminum interface. Based on this profile, an estimated elemental inter-mixing region of approximately 1.7 μm is visualized.

The mechanical properties of the typical RailClad transition joints showed a tensile strength of 152 MPa (population of 762 samples with 9.74 standard deviation). While the shear strength obtained is around 93 MPa (population of 1524 samples with 3.12 standard deviation). The tensile test specimens used are machined in the form of a cup in such way that the applied force is perpendicular to the plane of the interfaces between the aluminum and the steel.

Microhardness measurements have been made on this TJ combination. Fig. 4 shows a typical plot of the variations in hardness across the two interfaces. These results are expected for the as clad material, and the increase in hardness of the steel near the interface is product of the high deformation plus intermixing of elements in that region.

Typical mechanical properties of the alloys used for the explosion welding of the transition joint used in this study is shown in Table 1.

2. Materials and methods

2.1. Traction fatigue tests with normal compression on the joint plane

The main difficulty of fatigue tests on plates assembled by explosion welding is to design a specimen that allows for a normal stress on the joint plane of an area sufficiently representative of the welded junction. The welded interface has a unidirectional waveform giving an anisotropic behavior to the interface itself. Karolczuk et al. [5] used standard T-bone specimens but the stress was parallel to the interface, which does not correspond to the load case of this study. The design of the specimens was chosen so the allowed stress is in tension and in compression to perform fatigue tests with negative charge ratio. The drawing of the test specimen used to carry out the fatigue tests is presented in Fig. 5. The specimen has an axisymmetrical shape making it possible to have an accurate result by allowing the initiation of the fatigue crack in all orientations. A test fixture holds the S355 steel flange of the specimen while a punch applies axial fatigue loads in tension and compression using a screw and a thick washer, Fig. 6.

The tests were carried out on a servohydraulic pilot fatigue machine equipped with a load cell with a capacity of ± 100 kN, at ambient temperature and in air. The test machine was run to obtain a force following a sinusoidal signal of frequency 30 Hz. The stopping criter-

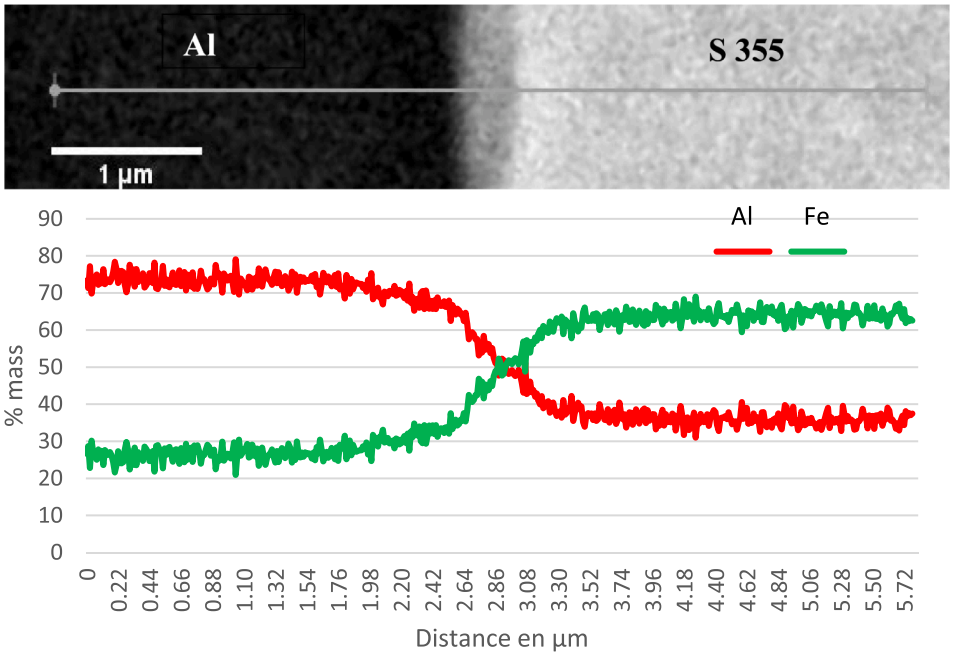

Fig. 3. Typical elemental profile at the boundary between the Al 1050 aluminum and S355 steel of a transition joint showing the zone of intermixing of elements.

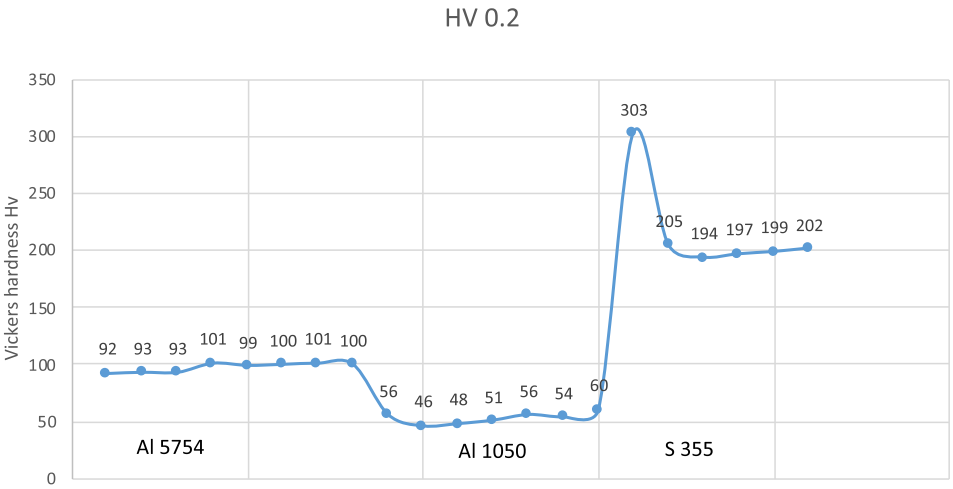

Fig. 4. Vickers microhardness values across the alloys of the transition joint S355/Al 1050/Al 5754 produced by explosion welding, showing a large increase in the hardness in the steel side near the Al 1050 interface.

Table 1
Typical mechanical properties of alloys used for the Transition Joint in this study.

Alloys of the TJ	Yield Strength, MPa	Tensile Strength, MPa	Elongation, %
S355 Steel	355 min	470 min	18 min
Al 5754 (H111)	80 min	190 min	18 min
Al 1050 (H14)4	85 min	100 min	12 min

ions were either an increase in the maximum displacement of one millimeter in the cylinder of the test machine, corresponding to a loss of stiffness and therefore rupture of the test piece, or a no-failure of the test piece to 10 million cycles.

2.2. Torsion fatigue tests

Torsion fatigue tests were carried out on test pieces as shown in Fig. 7. This design was used to be able to characterize the fatigue strength in pure shear stress of the welded junction. The test piece has a useful section identical to that of the tensile-compression test pieces, making it possible to have the same representative surface, and possibility of initiating the fatigue crack in all orientations with respect to the direction of the interface.

The tests were carried out on a servohydraulic fatigue machine equipped with a load cell with a capacity of ± 2.5kN.m. The tests were carried out at ambient temperature and in air. The force applied followed a sinusoidal signal of frequency 20 Hz. The stopping criterions were either an increase in the maximum angular displacement of three

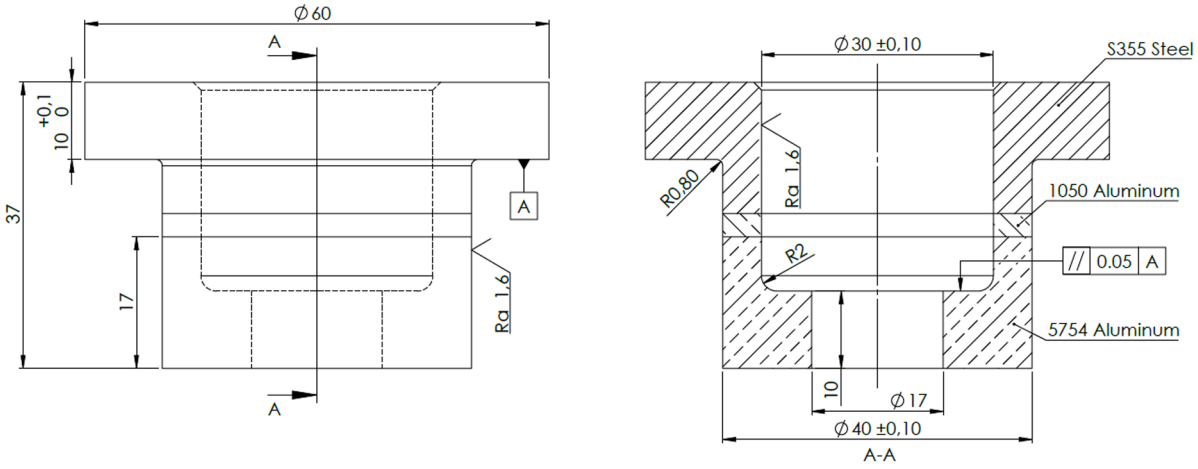

Fig. 5. Drawing of the traction/compression specimen used in this study.

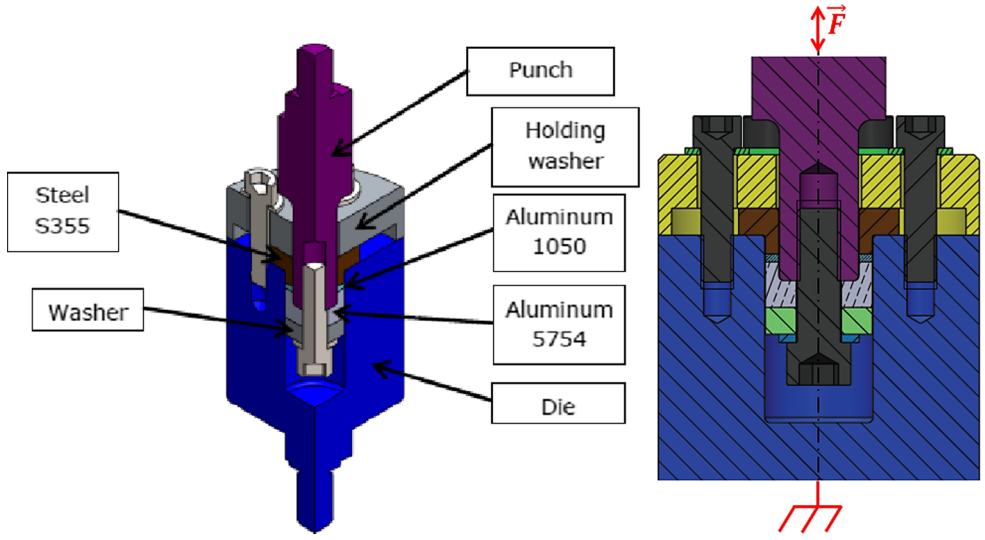

Fig. 6. Quarter sectional view of the test setup with the specimen, showing the "cup" type geometry of the sample.

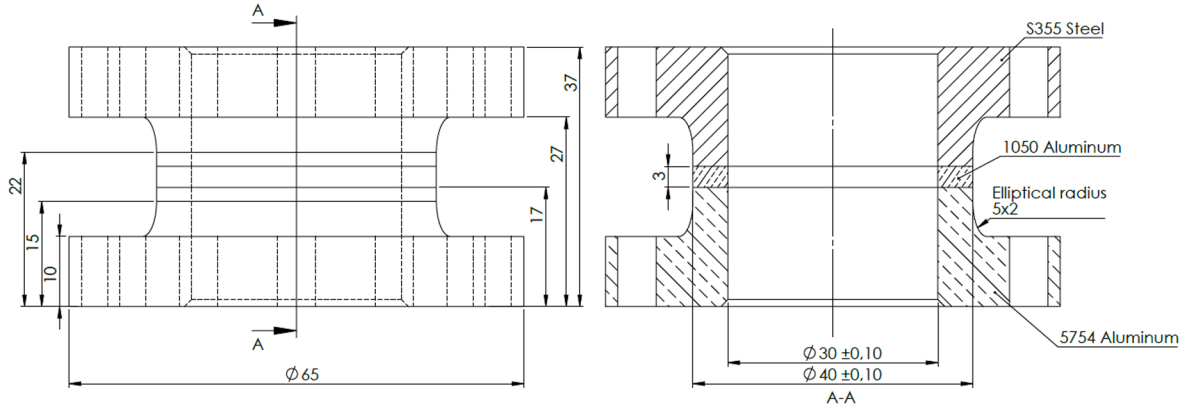

Fig. 7. Design of the torsion fatigue test specimens, where the Al 1050 interlayer between the S355 steel and the Al 5754 can be seen.

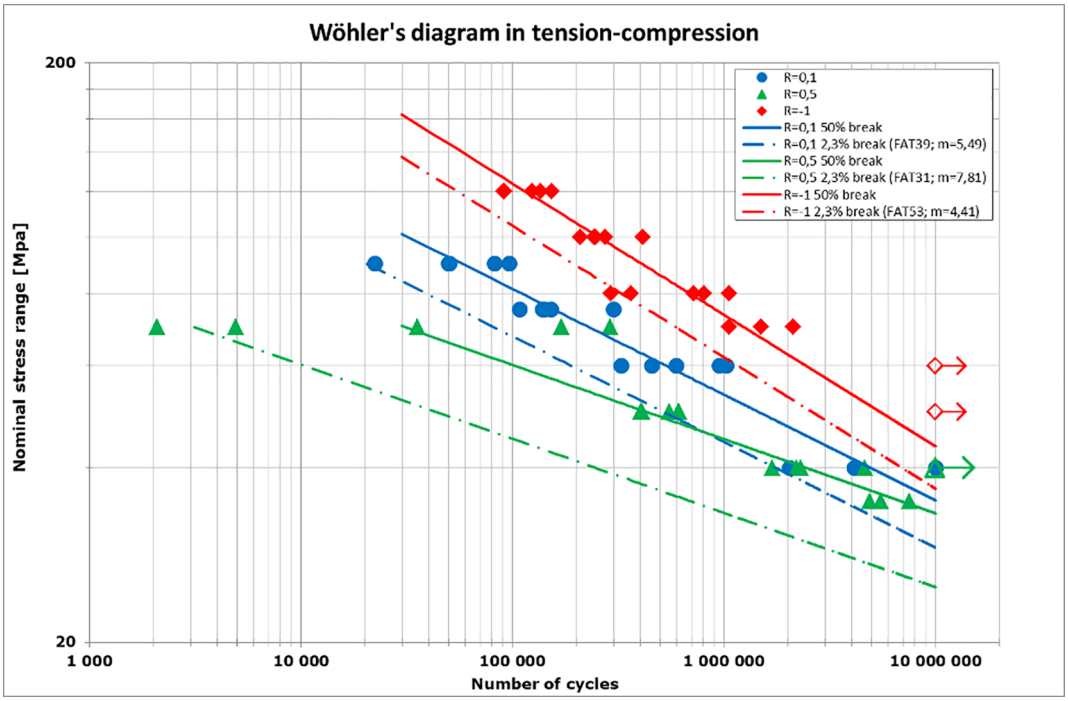

Fig. 8. Wöhler diagram in traction/compression for a S355/Al 1050/Al 5754 transition joint produced by explosion welding. The Basquin model, Eq. (1), is the best fit to represent the fatigue behavior of this explosion-welded joint.

Table 2
Basquin model parameters for behavior in traction/compression for a S355/Al 1050/Al 5754 transition joint produced by explosion welding.

Fracture probability[%]	Load ratio	C	m
50	0.5	18.89	7.81
50	0.1	15.48	5.49
50	−1	14.23	4.41
2.3	0.5	17.90	7.81
2.3	0.1	15.03	5.49
2.3	−1	13.90	4.41

degrees, corresponding to a loss of stiffness and consequently breaking of the test specimen, or a non-rupture of the test specimen at 10 million cycles.

3. Results

3.1. Fatigue tests in Traction/Compression normal to the joint

Four stress levels with the use of five test pieces per stage were tested for three different load ratios, R = 0.5, 0.1 and −1. The results of these tests are shown in a Wöhler diagram, Fig. 8 (Table A in Appendices). The dots with the arrows represent the results of unbroken samples at 10 million cycles.

$$Log\backslash;N = C - -m \quad Log\backslash;\Delta\sigma \tag{1}$$

The model parameters are given in Table 2 for the three load ratios and for 50% and 2.3% probabilities of failure, the latter being the equivalent of the FAT curve of the IIW recommendations [9]. The French Norm NF A03-405 “Essais de Fatigue-Traitement statistique des données” was used for this purpose. The results also make it possible to draw the Goodman-Smith diagram, Fig. 9. Most of the breaks occurred at the interface between S355 steel and Al 1050 aluminum (99.9%). The macrostructural features of the fracture face have a wave morphology which shows that the fatigue failure propagated at that interface, Fig. 10. Using scanning electron microscopy (SEM) it was possible to identify the zone of initiation of the crack located at the interface S355/Al 1050 on the outside surface of the test piece, Fig. 11. Both brittle and ductile fractures can be observed due to plastic deformation of the aluminum and more brittle fracture of the inter-mixed region of elements from the steel and aluminum,

3.2. Fatigue tests under torsion

The same test procedure as before was used for the torsion tests. The first tests carried out at a load ratio of R = 0.5 were inconclusive. The loading led directly to the plasticization of the specimen, specifically the aluminum layer of Al 1050. The first charge ratio was then lowered to R = 0.3. The results are reported in the Wöhler diagram in Fig. 12 (Table B in Appendices) with the plot of Basquin models with parameters given in Table 3. From this data, the Goodman-Smith diagram was produced as shown in Fig. 13 with truncations by the elastic limit of aluminum alloy Al 1050. This diagram explains the fact that fatigue tests with a load ratio R = 0.5 were inconclusive. In the case of shear fatigue tests, the interface Al 1050/Al 5754 broke, contrary to what was observed in the case of tensile-compression fatigue. This is confirmed by the observation of a longer wavelength characteristic of the interface Al 1050/Al 5754 as seen in Fig. 14. A hypothesis of what is happening will be described in section 4.2.

4. Discussion

4.1. Results from Traction/Compression tests

The results of tensile/compression tests are compared with the

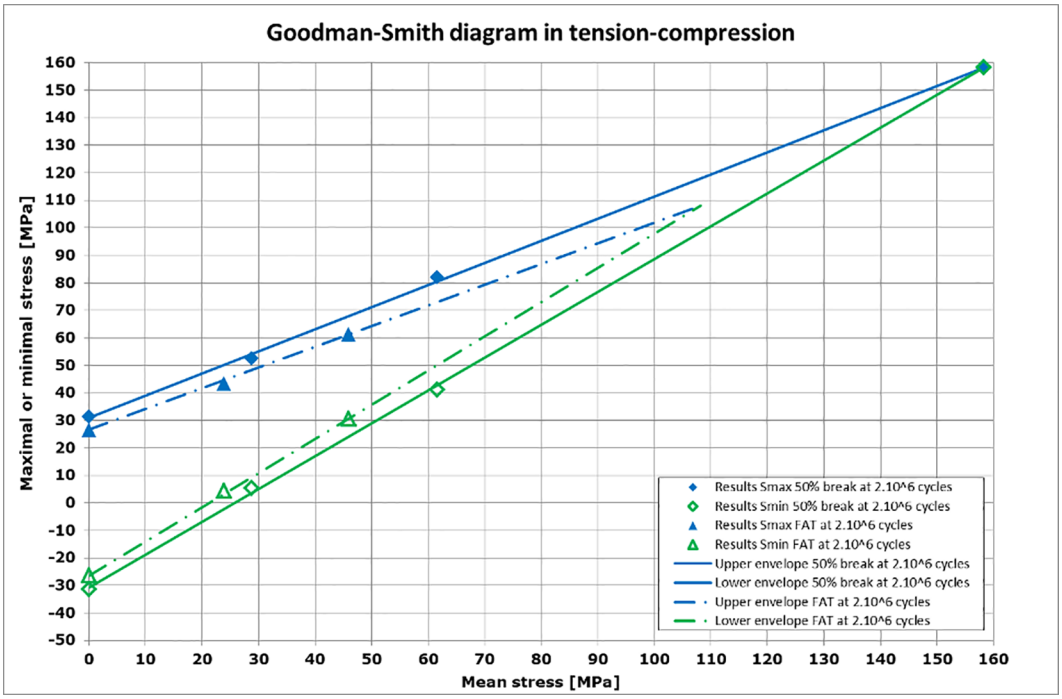

Fig. 9. Goodman-Smith diagram in traction/compression for a S355/Al 1050/Al 5754 transition joint produced by explosion welding.

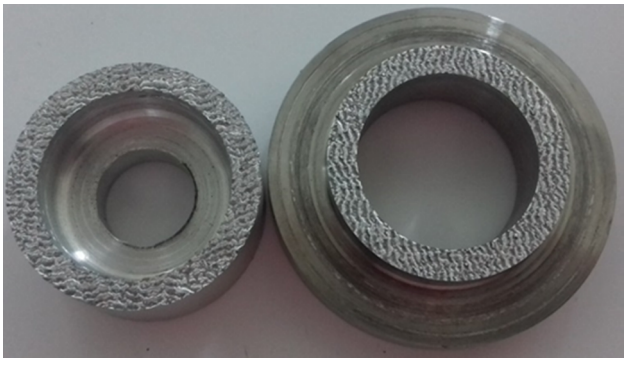

Fig. 10. Overall view of a typical fracture surface of a broken test piece under tension for a S355/Al 1050/Al 5754 transition joint produced by explosion welding. This particular one with a nominal stress amplitude of 50 MPa, R = 0.5, and n = 551,042.

curves given by the IIW recommendations for an aluminum butt welded joint, leveled and 100% controlled by non-destructive testing (NDT) (i.e. a fatigue class FAT45 for a load ratio R = 0.5) and shown in Fig. 15.

The behavior of the welded junction at first seems weaker than that of a butt weld at low number of cycles but the behavior changes as it approaches 10 million cycles. To understand why the results seem unfavorable at low number of cycles, we carried out a finite element analysis on the specimen to determine the influencing factor of the specimen geometry on the results. The entire test setup was considered in the finite element calculation to consider the influence of its stiffness. For the Finite Element Analysis (FEA) certain conditions were considered:

- Symmetry on cut areas (quarter section shown on Fig. 6);
- Flat contact under the die;
- Application of a load reference according to Table 4, corresponding to a stress range of 100 MPa. The negative sign corresponds to a

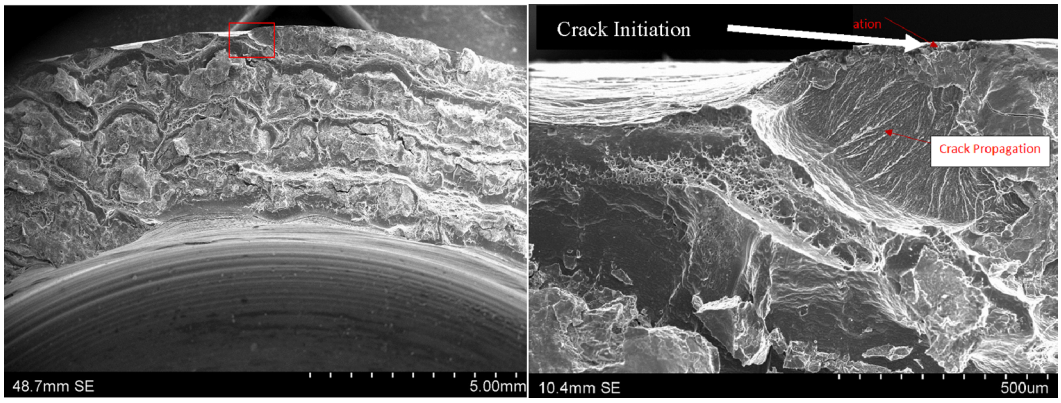

Fig. 11. SEM observation of fatigue crack initiation of sample shown in Fig. 8. Mixtures of ductile and brittle fractures are observed and expected due to the presence of intermixed elements.

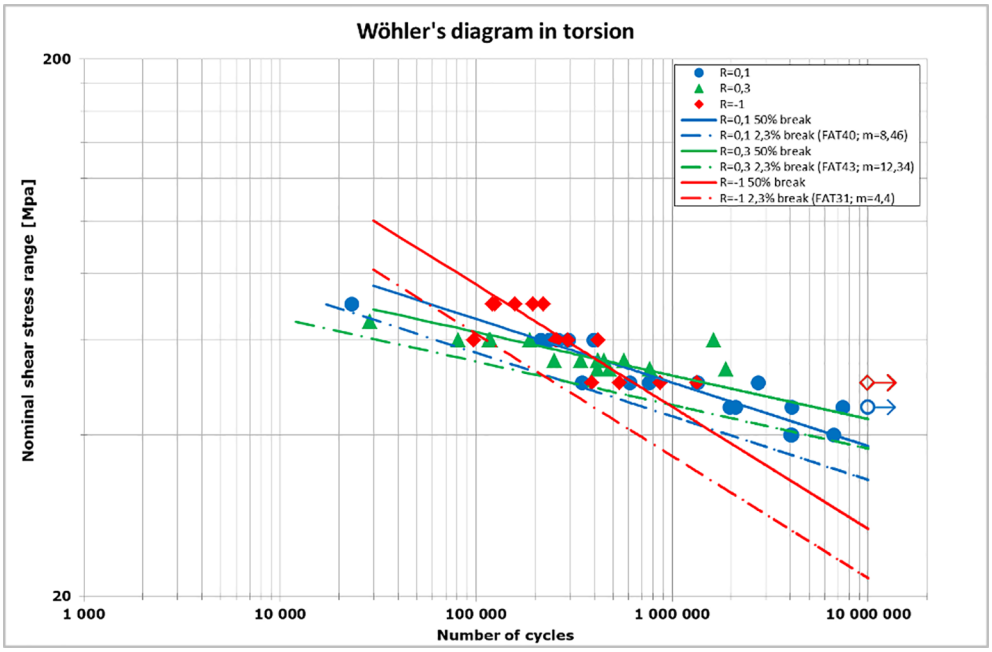

Fig. 12. Wöhler diagram in torsion for a S355/Al 1050/Al 5754 transition joint produced by explosion welding.

Table 3
Basquin model parameters for behavior in shear stress for a S355/Al 1050/Al 5754 transition joint produced by explosion welding.

Fracture probability[%]	Load ratio	C	m
50	0.3	27.14	12.34
50	0.1	20.37	8.46
50	−1	13.27	4.4
2.3	0.3	26.46	12.34
2.3	0.1	19.84	8.46
2.3	−1	12.87	4.4

compression of the punch resulting in a pull on the specimen;
- Glue global contact;
- Management of the contact between the specimen and assembly by non-penetrating;
- Mesh characteristics:
  - o Quadratic tetrahedral type mesh.
  - o Number of elements: 151,865.
  - o Max element size: 5 mm.
- Materials properties used (isotropic):
  - o Steel S355: Young's modulus, 210 GPa and Poisson's ratio, 0.28;

Fig. 13. Goodman-Smith diagram in shear stress for a S355/Al 1050/Al 5754 transition joint produced by explosion welding.

Fig. 14. Overall view of the typical fracture surfaces of the broken torsion specimen for a S355/Al 1050/Al 5754 transition joint produced by explosion welding. In this particular case, a nominal torsional stress amplitude of 50 MPa was used with R = 0.1, n = 761,311.

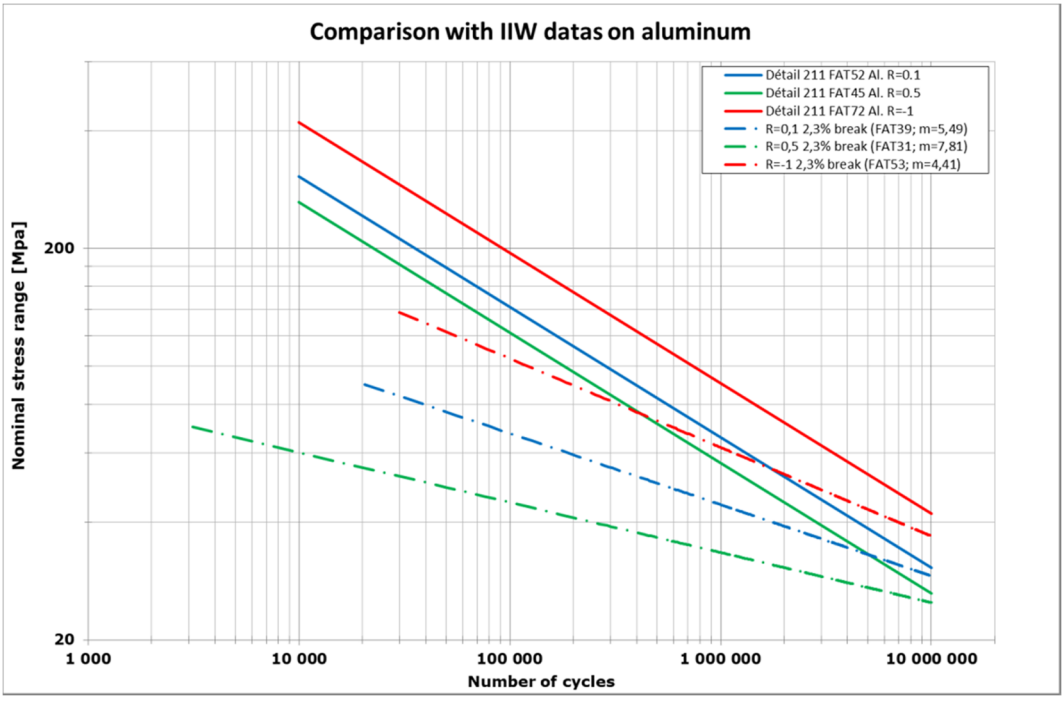

Fig. 15. Comparison of results of traction/compression with IIW recommendation for a S355/Al 1050/Al 5754 transition joint produced by explosion welding.

Table 4
Load cases considered for the FEA model.

Load Case	Description	Load Applied (N)
Case #1	Fmax at R = 0.1	−15,272
Case #2	Fmin at R = 0.1	−1,527
Case #3	Fmax at R = -1	−6,872
Case #4	Fmin at R = -1	6,872

- o Aluminum 1050: Young's modulus, 70 GPa and Poisson's ratio, 0.39;
- o Aluminum 5754: Young's modulus, 70 GPa and Poisson's ratio, 0.39;

The results of the calculations are given in Fig. 16. We note that the stress is not distributed homogeneously throughout the calibrated section. The local stress at the S355/Al 1050 interface is 50% higher on the external surface of the specimen than the nominal stress applied to the

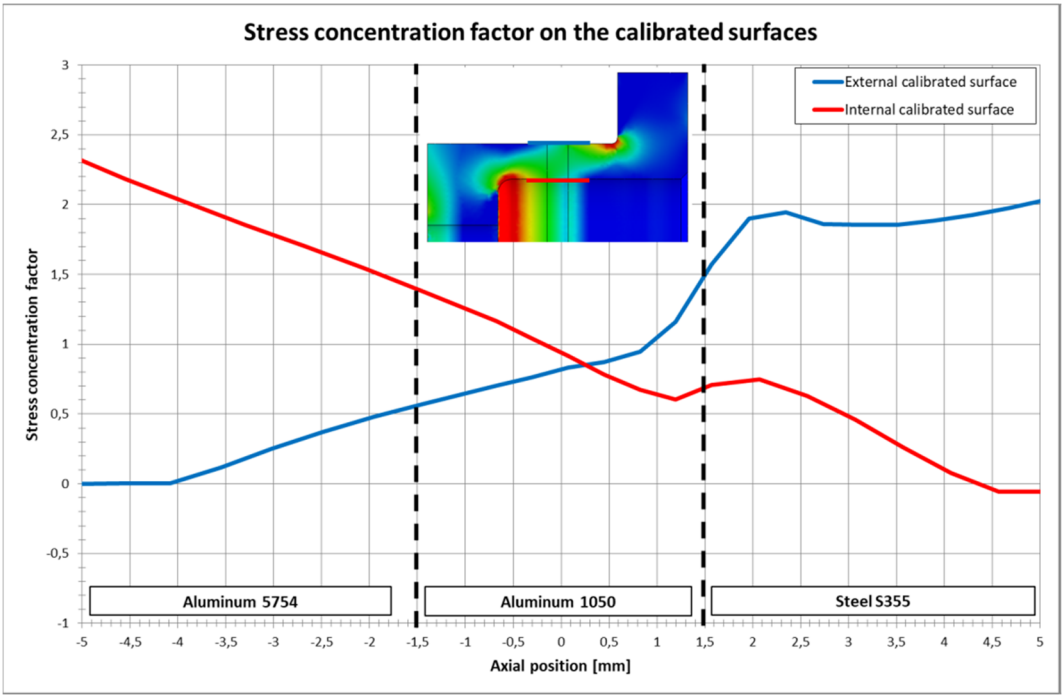

Fig. 16. Internal and external surface stress concentrations of the traction/compression specimen for a S355/Al 1050/Al 5754 transition joint produced by explosion welding.

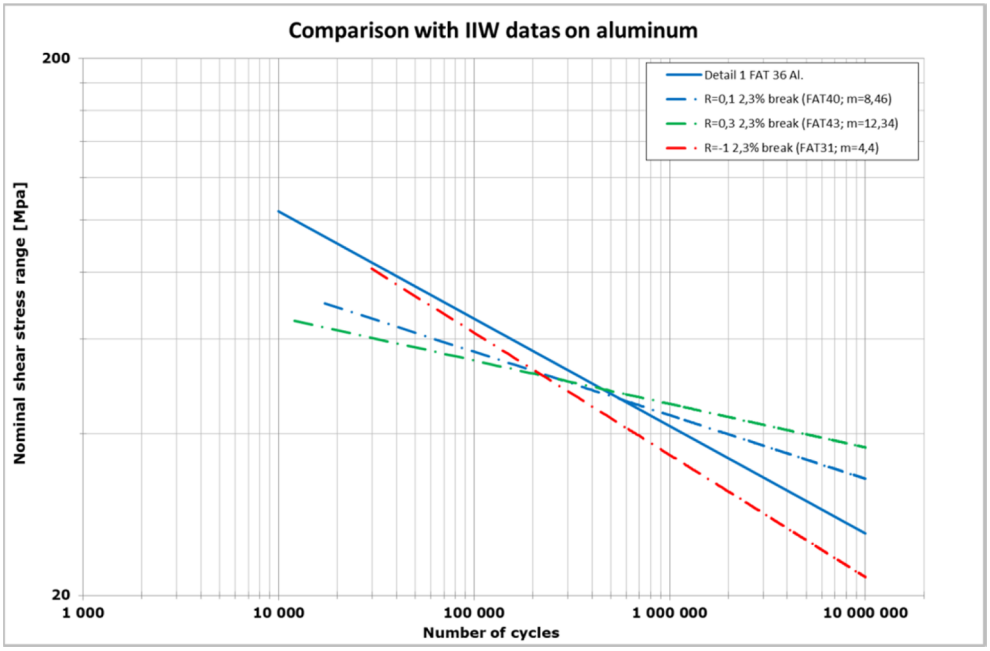

Fig. 17. Comparison of between shear stress results and IIW recommendation for a S355/Al 1050/Al 5754 transition joint produced by explosion welding.

calibrated section. This difference explains both the fatigue crack initiation site and the fact that the results are inferior to those of the IIW recommendations. The effect of the load ratio is the same in both cases.

4.2. Results from shear stress tests

The shear stress results are also compared to the curve given by the IIW recommendations for an aluminum butt welded joint, leveled and

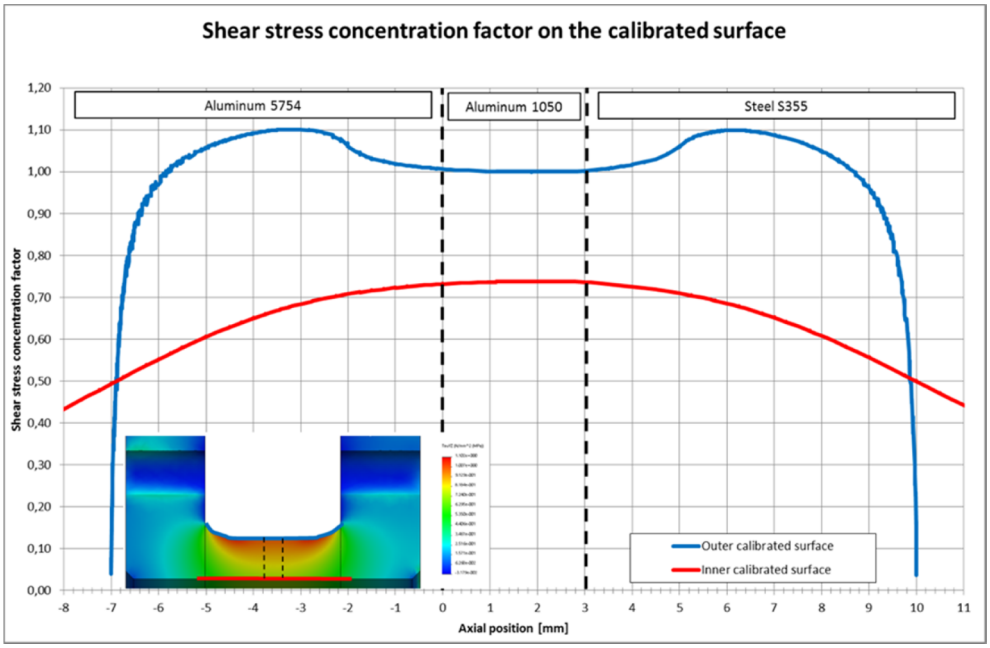

Fig. 18. Internal and external surface stress concentrations of the shear stress specimens for a S355/Al 1050/Al 5754 transition joint produced by explosion welding.

100% controlled by non-destructive testing (NDT) (i.e. a fatigue class FAT36) as seen in Fig. 17. The slopes of models at R = 0.1 and R = 0.3 are very close, while the slope for R = -1 is significantly different. The authors speculate that the reason for this behavior is due to the complex nature of the stresses that form at a wavy explosion bonded interface when R is negative. The stress field is significantly different at each point of the wave, whether at a "hill" or "valley", or when at the maximum slope of that wave. The authors recommend that a more detailed study would be needed to corroborate this hypothesis. The fatigue in shear is close to that given by the recommendations of the IIW. No information is available on the effect of the load ratio for butt welds. In the case of our experimental results, the effect of the load ratio results in a change of slope of the Basquin model is seen. The effect of the load ratio is therefore not zero as is generally observed for base metals. Fig. 18 shows the calculated internal and external surface stress concentrations of the torsion specimens.

5. Conclusions

From the tests carried out on an explosion-welded steel-aluminum junction, we can draw the following conclusions:

- The experimental tensile/compressive fatigue results show a 25–32% reduction in the fatigue class compared to the IIW data for a flared, flawless butt weld. This difference is explained by the stress concentration generated by the geometry of the specimen, increasing the nominal stress by approximately 50%. However, the higher slope coefficient of the fatigue curve makes it possible to obtain lifetimes substantially equivalent to the recommendations of the IIW at 10 million cycles;
- The effect of the load ratio for tensile/compressive fatigue is in accordance with IIW recommendations;
- Shear fatigue results are close to IIW recommendations. The finite element calculation of the specimen confirms that the local shear stress in the calibrated zone is equal to the nominal shear stress. This allows us to say that the shear fatigue strength of the explosion-welded junction tested in this study is equivalent to a traditional butt welded joint;
- The load ratio does not normally affect shear fatigue. In the case of explosion welded junctions, the load ratio influences the slope of the Basquin model and therefore slightly modifies the Goodman-Smith diagram. The waveform interface is probably influencing this phenomenon, where the stress fields constantly changes depending on the location within the wave.

Declaration of Competing Interest

The authors declare that they have no known competing financial interests or personal relationships that could have appeared to influence the work reported in this paper.

Appendix

(See Tables A1 and B1)

Table A1
Results of tests in traction/compression.

Specimen identity	Id [mm]	Od [mm]	$\Delta\sigma_N$[MPa]	Load ratio	Number of cycles
4.1	29.99	40.08	40	0.1	2 047 392
4.2	30.04	40.14	60	0.1	595 229
4.3	30.00	40.10	60	0.1	456 088
4.4	29.96	40.13	90	0.1	82 123
4.5	30.05	40.06	90	0.1	49 743
4.6	30.04	40.04	90	0.1	22 374
4.7	30.05	40.08	40	0.1	4 135 874
5.1	30.01	40.07	60	0.1	326 056
5.2	30.01	40.09	60	0.1	1 025 769
5.3	30.02	40.09	60	0.1	949 632
5.4	29.98	40.06	90	0.1	96 804
5.5	30.04	40.08	90	0.1	50 274
5.6	30.00	40.06	40	0.1	9 999 900
5.7	30.04	40.08	75	0.1	108 402
6.1	30.04	40.03	75	0.1	152 042
6.2	30.03	40.02	75	0.1	300 629
6.3	30.05	39.98	75	0.1	139 050
6.4	30.01	40.02	75	0.1	141 764
6.5	30.03	40.00	50	0.5	551 042
6.6	30.03	39.99	70	0.5	289 471
4.9	30.10	40.15	70	0.5	170 661
4.10	30.04	40.04	50	0.5	402 770
4.11	30.04	40.02	70	0.5	4 900
4.12	30.08	39.95	50	0.5	612 462
4.13	30.04	40.08	35	0.5	4 868 145
4.14	30.06	40.10	50	0.5	605 641
4.15	30.09	40.04	70	0.5	2 085
4.16	30.01	40.05	35	0.5	5 527 653
4.17	30.01	39.92	40	0.5	4 628 752
4.18	30.09	40.01	40	0.5	1 685 260
4.19	30.05	40.04	40	0.5	2 297 773
4.20	30.00	39.99	40	0.5	2 198 200
5.9	30.05	39.95	40	0.5	10 000 000*
6.13	30.02	39.98	35	0.5	7 509 178
6.18	29.99	39.93	50	0.5	409 578
6.19	29.99	39.98	70	0.5	35 496
5.10	30.05	39.99	80	−1	718 014
5.11	30.01	39.92	80	−1	292 097
5.12	29.96	39.94	80	−1	1 054 314
5.13	30.05	40.00	80	−1	804 244
5.14	30.01	40.03	100	−1	411 885
5.15	29.97	39.99	100	−1	246 824
5.16	30.05	40.02	100	−1	208 764
5.17	30.01	40.04	100	−1	275 440
5.18	29.97	39.96	50	−1	10 000 000*
5.19	30.03	39.98	120	−1	90 549
5.20	29.99	39.98	120	−1	91 639
6.8	29.99	40.05	120	−1	135 280
6.9	30.00	39.96	120	−1	123 750
6.10	30.00	40.01	120	−1	153 285
6.11	30.01	40.00	80	−1	362 851
6.12	30.00	40.01	100	−1	243 241
6.14	30.11	40.06	60	−1	10 000 000*
6.15	29.96	39.96	70	−1	1 056 677
6.16	29.95	39.97	70	−1	2 124 467
6.17	29.98	39.93	70	−1	1 494 472

* Non-break.

Table B1
Results of fatigue tests in torsion.

Specimen identity	Id [mm]	Od [mm]	$\Delta\tau_N$[MPa]	Load ratio	Number of cycles
1.1	30.04	39.98	40	0.1	6 693 621
1.3	30.04	39.80	70	0.1	23 254
1.4	30.01	39.80	60	0.1	398 834
1.5	30.07	39.85	60	0.1	261 751
1.6	30.09	39.84	50	0.1	761 311
1.7	30.07	40.02	60	0.1	214 180
2.1	30.03	40.08	50	0.1	609 680
2.2	30.00	40.02	60	0.1	235 409
2.3	30.01	39.98	50	0.1	346 413
2.4	30.06	40.05	60	0.1	297 018
2.5	30.03	40.01	50	0.1	1 345 148
2.6	30.06	40.06	40	0.1	4 007 425
2.7	30.04	40.00	50	0.1	2 745 770
3.1	29.97	39.99	45	0.1	2 111 475
3.2	30.04	39.97	40	0.1	4 075 828
3.6	30.00	40.00	45	0.1	4 077 013
3.4	30.03	39.90	45	0.1	7 445 342
3.5	30.05	40.02	45	0.1	1 971 115
1.9	30.02	40.05	45	0.1	10 000 000*
2.20	29.95	39.97	50	0.3	10 000 000*
3.9	29.95	40.00	60	0.3	1 627 555
3.11	29.98	39.92	60	0.3	118 796
3.12	29.90	40.03	60	0.3	80 999
3.13	29.96	39.90	65	0.3	28 805
3.14	29.94	39.94	55	0.3	570 310
3.15	29.94	39.93	55	0.3	451 046
3.16	30.07	40.01	55	0.3	250 278
3.17	30.04	39.93	53	0.3	771 565
3.18	30.04	39.98	55	0.3	416 056
3.19	30.06	39.93	60	0.3	188 375
3.20	30.04	39.91	53	0.3	1 875 827
3.8	30.05	39.91	53	0.3	417 550
3.3	30.03	39.95	55	0.3	420 622
1.8	30.08	39.90	60	0.3	116 461
2.8	30.04	39.94	55	0.3	342 679
3.7	30.06	39.80	53	0.3	476 594
1.12	29.96	40.07	60	−1	293 959
1.13	29.97	40.05	70	−1	195 653
1.14	30.00	40.08	70	−1	124 939
1.15	29.97	40.03	70	−1	158 098
1.16	29.97	40.00	70	−1	121 117
1.17	29.94	40.01	70	−1	220 097
1.19	29.97	40.01	50	−1	389 900
1.20	29.97	40.04	50	−1	1 341 281
2.9	29.97	40.10	50	−1	865 926
2.11	30.00	39.99	50	−1	540 492
2.12	29.90	39.97	50	−1	10 000 000*
2.13	29.97	39.92	60	−1	420 072
2.14	30.03	40.01	60	−1	259 444
2.15	29.97	40.00	60	−1	97 098
2.16	29.92	39.99	60	−1	254 371
2.17	29.92	40.00	45	−1	10 000 000*
2.18	29.93	40.01	50	−1	371 863
2.19	29.92	40.01	47	−1	10 000 000*

* Non-break.

References

[1] Young G, Banker J. Explosion welded, bi-metallic solution to dissimilar metal joining. In: Proceedings of the 13th offshore symposium 2004, February 24, Houston, Texas, Texas Section of the Society of Naval Architects and Marine Engineers. p. 6.

[2] Akbari Mousavi SAA. Farhadi Sartangi P. Effect of post-weld heat treatment on the interface microstructure of explosively welded titanium–stainless steel composite. Mater Sci Eng 2008;494:329–36.

[3] Acarer Mustafa, Demir Bilge. An investigation of mechanical and metallurgical properties of explosive welded aluminum–dual phase steel. Mater Lett 2008;62(25):4158–60.

[4] Zhou, B. bin; Zhou, C. yu; Chang, L.; Yu, X. chun; Ye, C.; Zhang, B. jun: Investigation on fatigue crack growth behavior of Zr702/TA2/Q345R explosive welding composite plate with a through-wall crack. Compos. Struct. 2020, 236, 111845.

[5] Karolczuk A, Kowalski M, Banski R, Zok F. Fatigue phenomena in explosively welded steel-titanium clad components. Int J Fatigue 2013;48:101–8.

[6] Borisenko VA, Berezovskii LB, Levchenko VA, Kozhevnikov VE, Sannikov VI. Special features of failure of bimetal in low-cycle fatigue. Strength Mater 1984;16(1):25–7. https://doi.org/10.1007/BF01530180.

[7] Jiang F, Zhao K, Sun J. Evaluation of interfacial crack growth in biomaterial metallic joints loaded by symmetric three-point bending. Int J Pressure Vessels Piping 2003;80:129–37.

[8] Hobbacher A. Recommendations for Fatigue Design of Welded Joints and Components. IIW-document XIII-2460-13.

[9] S. Liu, J. Banker, and C. Prothe, Explosion Welding, Welding Fundamentals and Processes, Vol 6A, ASM International, 2011.

[10] Bataev I, Lazurenko D, Tanaka S, Hokamoto K, Bataev A, Guo Y, et al. High cooling rates and metastable phases at the interfaces of explosively welded materials. Acta Mater. 2017;135:277–89.

[11] Liu S, Prothe Curtis, Banker John, Parish C, Kenik E. Explosive Weld Interface Characterization - Complex Microstructure & Solidification Details. Microsc Microanal 2012;18:1674–5.

[12] McKenney CR, Banker J. Explosion-bonded metals for marine structural applications. Marine Technology Society of Naval Architects and Marine Engineers. 1971. p. 285–92.
[13] MIL-J-24445A, Military Specification: Joint, Bimetallic Bonded, Aluminum to Steel (25 JUL 1977).
[14] Moore, S. and Banker, J, "Aluminum Steel Construction in a New 36M [120 Ft] Patrol Boat"; Proceedings of the Ship Production Symposium, held in New Orleans, Louisiana, on 2-4 September 1992.
[15] Ranker, J.G. and Gaines E-T., "Shipboard Aluminum/Steel Welded Transition Joints Evaluation and Improvements," 1990 Ship Production Symposium, Milwaukee, WI, sponsored by Society of Naval Architects and Marine Engineers.
[16] Ranker, J.G. and Gaines E.T. "Shipboard Aluminum/Steel Welded Transition Joints, " 1991 Ship Production Symposium, San Diego, CA, sponsored by Society of Naval Architects and Marine Engineers.